Acquiring tomographic images from panoramic X-ray scanners

Van-Giang Nguyen[a], Soo-Jin Lee[b]
[a]Department of Information Systems, Le Quy Don Technical University, Hanoi, Vietnam;
[b]Department of Electronic Engineering, Paichai University, Daejeon, Republic of Korea

ABSTRACT

We propose a new method to acquire three-dimensional tomographic images of a large object from a dental panoramic X-ray scanner which was originally designed to produce a panoramic image of the teeth and jaws on a single frame. The method consists of two processes; (i) a new acquisition scheme to acquire the tomographic projection data using a narrow detector, and (ii) a dedicated model-based iterative technique to reconstruct images from the acquired projection data. In conventional panoramic X-ray scanners, the suspension arm that holds the X-ray source and the narrow detector has two moving axes of the angular movement and the linear movement. To acquire the projection data of a large object, we develop a new data acquisition scheme that can emulate an acquisition of the projectional view in a large detector by stitching narrow projection images, each of which is formed by a narrow detector, and design a trajectory to move the suspension arm accordingly. To reconstruct images from the acquired projection data, an accelerated model-based iterative reconstruction method derived from the ordered subset convex maximum-likelihood expectation-maximization algorithm is used. In this method each subset of the projection data is constructed by collecting narrow projection images to form emulated tomographic projectional views in a large detector. To validate the performance of the proposed method, we tested with a real dental panoramic X-ray system. The experimental results demonstrate that the new method has great potential to enable existing panoramic X-ray scanners to have an additional CT's function of providing useful tomographic images.

Keywords: panoramic imaging, CT image reconstruction, dental imaging, X-ray imaging

1. INTRODUCTION

Dental panoramic radiography, also called panoramic X-ray, has long been used to image all the teeth and nearby structure at a time. The two-dimensional (2D) panoramic image shows the structure along a predefined curve in the patient jaw. In a panoramic X-ray system, the X-ray source and the detector are mounted to and fixed in two opposite sides of a suspension arm. The suspension arm is mounted onto a fixing and moving means (see Fig. 1) which allows the suspension arm to rotate and move around the object to be imaged in a special trajectory. The angular speed and linear movement speed of the arm are maintained so that the X-rays from the source to the detector are as perpendicular as possible to the dental arc to be imaged.

With the recent development of digital X-ray technology, there has been a growing interest in acquiring 3D information from panoramic X-ray. One representative method[1] is to utilize the traditional panoramic imaging technique that moves and rotates the detector and the X-ray source appropriately during the acquisition process so that a slice image can be acquired by bringing the regions of interest in a given plane into sharp focus while the regions far from the given plane are blurred. Repeating this procedure for several different planes will result in a set of slice images just like tomosynthetic images which contain cross-sectional information of the object. In this case, since the ordinary panoramic unit cannot be directly used, a modification of the unit is required.

Other methods[2,3,4] reprogrammed the panoramic unit to acquire projection data of the region of interest in the object from different view angles. In particular, a special scanning movement was designed to cover a large region of interest using narrow detector in the panoramic unit, followed by a procedure to synthesize the acquired narrow beam projection data into tomosynthetic images. These tomosynthetic images were then used for reconstructing 3D structure of the object[5]. Later in Ref. 6, to improve the quality of reconstruction, both the conventional panoramic data and the synthesized projection images were utilized.

Medical Imaging 2014: Physics of Medical Imaging, edited by Bruce R. Whiting, Christoph Hoeschen, Despina Kontos,
Proc. of SPIE Vol. 9033, 90332W · © 2014 SPIE · CCC code: 1605-7422/14/$18 · doi: 10.1117/12.2043232

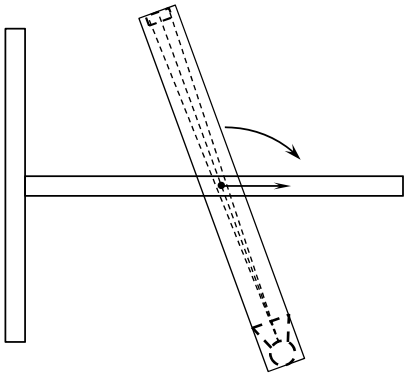

Fig. 1. A typical panoramic X-ray scanner. The suspension arm holding a pair of detector and X-ray source can rotate and move along an axis.

In this work, we propose a new method of acquiring cross-sectional tomographic images using a panoramic unit with a narrow detector. The crux of the method is how to design a special trajectory of the pair of the X-ray source and narrow detector in order to construct the conventional projection data from which the cross-sectional images can be directly reconstructed by a well-adapted model-based iterative reconstruction technique. Our method differs from the existing methods in that, rather than reconstructing from the synthesized tomosynthetic images, it reconstructs cross-sectional images directly from the original projection data. As a result, reconstructed images by using our method is close to the conventional CT images. Similar to the prior methods[2,3,4,5,6], our method is capable of providing cross-sectional images for a relatively large object using a narrow detector without the requirement of a large, expensive detector.

The remainder of this paper is organized as follows: Section 2 first describes our method to acquire projection data about an object using a narrow detector and then specifies how to apply the idea to a real panoramic scanner. This section also describes an iterative method to reconstruct images from acquired projection data. In Section 3 our experimental results that show the performance of our proposed methods are presented. Section 4 discusses our work and finally draws a conclusion.

2. METHODS

2.1 Acquiring projection image about a large object using a narrow detector

Since a typical panoramic X-ray scanner illustrated in Fig. 1 uses a narrow detector, to acquire the projection data that can provide cross-sectional images of a large object, it needs to repeatedly position the source and detector pair so that it can emulate the large detector of a conventional x-ray CT which covers the whole object in a single acquisition. (See Fig. 2(a).) Unfortunately, however, the desired acquisition scheme in Fig. 2(a) cannot be made with the panoramic scanner in Fig. 1 which has only two degrees of freedom, one linear movement and one angular movement.

In this work, the movement of the suspension arm is carefully adjusted (as shown in Fig. 2(b)) to cover the object in the minimal number of steps (each step acquires a sub-projection image) without any overlap between two adjacent steps yielding two sub-projection images. The requirement for non-overlap is very important to minimize non-uniform sensitivity for the region to be imaged. For a step-and-shoot mode, removing the overlap not only helps to reduce the artifact in reconstruction but also eliminates the redundant and harmful radiation passing through the patient. In Fig. 2(b) the actual center of rotation is always fixed in the axis (designated as the *transition axis*) of the fixing and moving means while the suspension arm rotates. The resulting projection image of the object is named the *irregular projection image*. (See Fig. 2(b).)

In order to acquire the irregular projection image, it is necessary to design a trajectory for moving the suspension arm appropriately. Figure 3 shows how to combine the linear and angular movements to move the suspension arm from the current position to the next position. Assume that the suspension arm is at the position where the currently mounted point is located at (C_x, C_y), the source is located at (S_x, S_y), the angle between the suspension arm and the linear movement

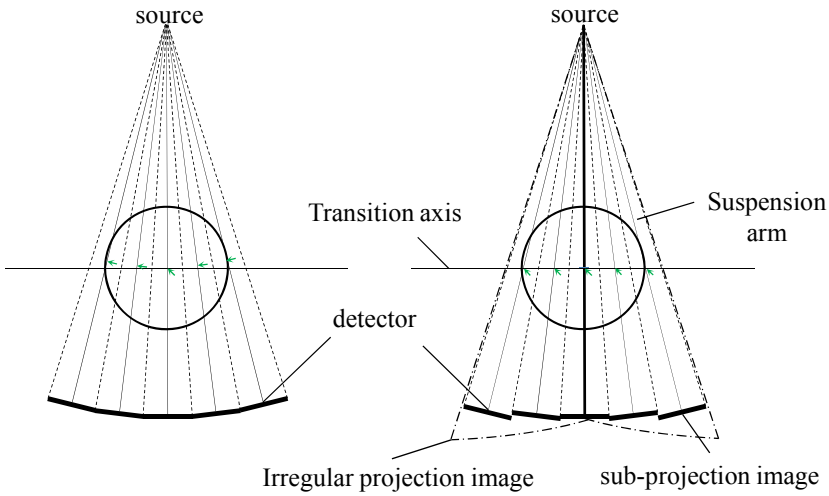

Fig. 2. Diagrammatic view of principle of the proposed method to acquire projection data of a large object using a narrow detector: (a) ideal model; (b) proposed model. The solid line connects the source and the center of detector. The dotted line denotes the area imaged by the detector. The dash-dotted line denotes the area imaged by the irregular projection image. Note that, for the ideal model, the center of rotation (designated by arrows) cannot be positioned on the transition axis.

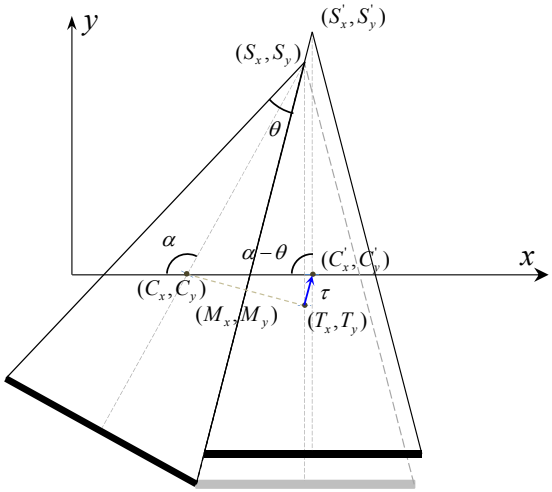

Fig. 3. A combination of angular and linear movements to move the suspension arm from one position to the next position.

axis is α, and θ is the fan angle formed by the detector-source pair. The procedure to move the suspension arm to the next position is then summarized as follows:

(i) Move (C_x, C_y) to the new position (T_x, T_y) by rotating the arm by the angle θ about the source position (S_x, S_y).

(ii) Compute the amount of the lift $\tau = -T_y / v_y$ along the direction of the vector (v_x, v_y) that directs from the midpoint between (C_x, C_y) and (T_x, T_y) (designated as (M_x, M_y)) to the original source position (S_x, S_y).

(iii) Move (T_x, T_y) and (S_x, S_y) to $(C_x', C_y') = (T_x + \tau v_x, T_y + \tau v_y)$ and $(S_x', S_y') = (S_x + \tau v_x, S_y + \tau v_y)$, respectively.

(iv) Move the position of the suspension arm parameterized by (α, C_x, C_y) to the new position with the new parameters $(\alpha - \theta, C_x', C_y')$.

Fig. 4. Simulated irregular projection image formed by our proposed method. (The image shows –log of the original one.)

In conventional panoramic scanners, given the parameters (α, C_x, C_y) for the old position and the new parameters $(\alpha - \theta, C_x^{'}, C_y^{'})$ for the new position, the physical movement according to the two sets of position parameters can be easily made.

Since an irregular projection image can be regarded as a projection image in a conventional CT scanner, via repeated acquisition processes at many different angles, it can be directly used as tomographic projection data from which cross-sectional images can be reconstructed.

Fig. 4 shows a modeled irregular projection image where it was constructed from 24 narrow projection segments, which can be used later to reconstruct the cross-sectional images about the object.

2.2 Sampling scheme in continuous mode

In practical panoramic imaging, while the detector records the data at every interval of $1/FR$ second where FR is the number of frames per second, the X-ray source continuously exposes radiation during the entire scan. (In the CdTe detector currently used in panoramic imaging, $FR \approx 200$.) Therefore, during the movement of the suspension arm from one position to the next position in Fig. 2(b), many rays continuously pass through the object by intrinsically producing many sub-projection images. Instead of giving up such free sub-projection images, we can make use of those images for reducing noise thereby improving the quality of reconstructed images. Assume that each sub-projection image has the view angle of θ and the object is fully covered by N sub-projection images. In that case, the angular movement of the suspension arm needed to construct an irregular projection image is $N\theta$. (Though the actual angular movement is $(N-1)\theta$, we acquire one more θ to ensure that all of the irregular projection images fully cover the object.) If the sampling interval of the detector movement (the gap between the two consecutive recording positions) is β, the total number of recorded sub-projection images is $\lfloor N\theta/\beta \rfloor$ which can produce $\lfloor \theta/\beta \rfloor$ irregular projection images. The resulting irregular projection images are formed as shown in Table 1 and illustrated in Fig. 5. Though the redundant projection images differ in a very small angle, they can be useful for reducing noise by averaging frames.

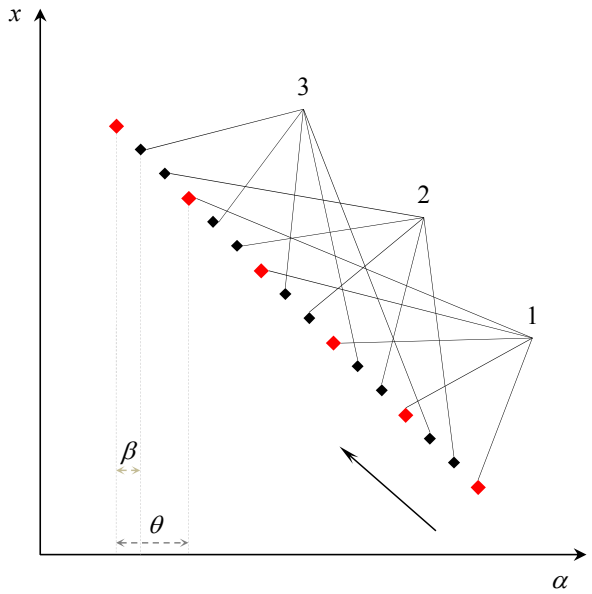

Fig. 5. Construction of irregular projection images in a continuous acquisition mode. x is the linear movement axis. α is the angular movement axis.

Table 1. Construction of irregular projection images in a continuous acquisition mode

Irregular projection image	Index of sub-projection image
1	$1,1+\lfloor\theta/\beta\rfloor,...,1+\lfloor(N-1)\theta/\beta\rfloor$
2	$2,2+\lfloor\theta/\beta\rfloor,...,2+\lfloor(N-1)\theta/\beta\rfloor$
…	
$\lfloor\theta/\beta\rfloor$	$\lfloor\theta/\beta\rfloor,\lfloor\theta/\beta\rfloor+\lfloor\theta/\beta\rfloor,...,\lfloor N\theta/\beta\rfloor$

2.3 Reconstruction algorithm

Though our proposed method directly reconstructs the images from the acquired projection data, due to the irregular movement of the source-detector pair, it does not provide the conventional projection data that can be directly reconstructed by the analytical reconstruction method based on the inverse Radon transform, such as the filtered backprojection method. This is mainly due to the fact that the irregular projection images are constructed by stitching several narrow projection segments. Without modeling the data formation process, images cannot be correctly reconstructed. In this work, to maximize the accuracy of reconstruction by taking the data formation process into account, a model-based iterative reconstruction (MBIR) method [7-9] is used. In particular, we consider an ordered-subsets (OS) version[9] of the MBIR method. In the OS method, the entire projection data are first subdivided into an ordered sequence of disjoint subsets. An iteration is then defined as a single pass through all the subsets. For each subset, the iterative method is performed and the reconstruction from this subset becomes the initial value in the next subset. In this work, the projection data are divided into subsets so that each subset corresponds to one or more consecutive irregular projection images depending on the total number of subsets used in the reconstruction process.

3. EXPERIMENTAL RESULTS

We applied our proposed method to a real dental panoramic X-ray scanner, Papaya^{TM}, manufactured by Genoray Co., Ltd (Seongnam, S. Korea). The scanner had the following parameter settings: the detector was of the size 150mm×4.8mm (1500×48 detector cells with the bin size of 0.1×0.1mm^2), the distance from the source to the detector was 480mm, and the distance from the source to the center of rotation was 330mm. We acquired 13 principal irregular projection images for our real data experiment (This corresponds to 13 different views in the conventional CT scanner).

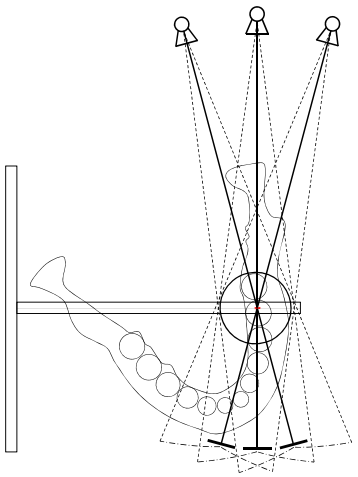

Fig. 6 Schematic diagram of the proposed method to acquire cross-sectional images of a molar region of the human jaw. The 13 principal projection images were used. (Only 3 are shown here).

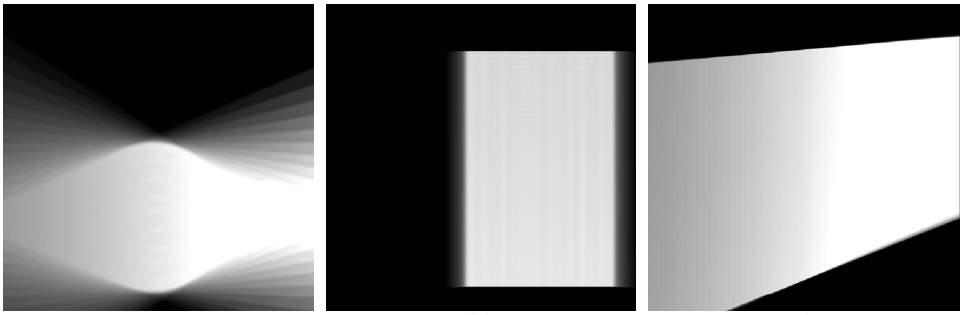

Fig. 7 Three-dimensional sensitivity map for the tested trajectory: (a) axial view; (b) sagittal view; (c) coronal view. The sagittal view is the view of interest.

With a given angular movement speed, the acquisition of each principal irregular projection image generated $\lfloor \theta / \beta \rfloor$ irregular projection images. In our work, with $\theta = 0.47745^\circ$ and $\beta = 0.01147^\circ$, the acquisition of each principal irregular projection image generated 42 irregular projection images (as shown in Table 1). Out of 42, we selected 12 irregular projection images for reconstruction. Therefore, there were a total of 156 irregular projection images. In practice, since dentists prefer to have cross-sectional slices along a given direction, we acquired the principal irregular projection images in the coverage angle of 60 degrees only. The acquisition time for each principal irregular projection image was 5 seconds. In particular, we aimed to obtain cross-sectional slices of the molar region of the human jaw (See Fig. 6). The tube potential was 75kV and the tube current was 8mA.

To observe the characteristic of the imaging system that uses our proposed acquisition scheme, we calculated a 3-D sensitivity map by performing backprojection of a uniform projection image into the 3-D imaging volume (In this work, we used Siddon's ray-tracing method[10] to perform backprojection). The sensitivity map in Fig. 7(b) shows that, despite the positional irregularity of the source-detector pair as shown in Fig. 2(b), it is almost uniform in the region of interest to be imaged.

To test our method, we physically acquired projection data from a head phantom. Fig. 8 shows 13 selected irregular projection images (one per each principal irregular projection image) where each irregular projection can be regarded as the projection image acquired from one large detector. Due to the non-uniformity in the sensitivity of the detector cells along the border of the two adjacent blocks and near the border of the detector, the projection images contain some distortions in the boundaries in between the adjacent detectors. (The images shown here are the raw data before any calibration process.)

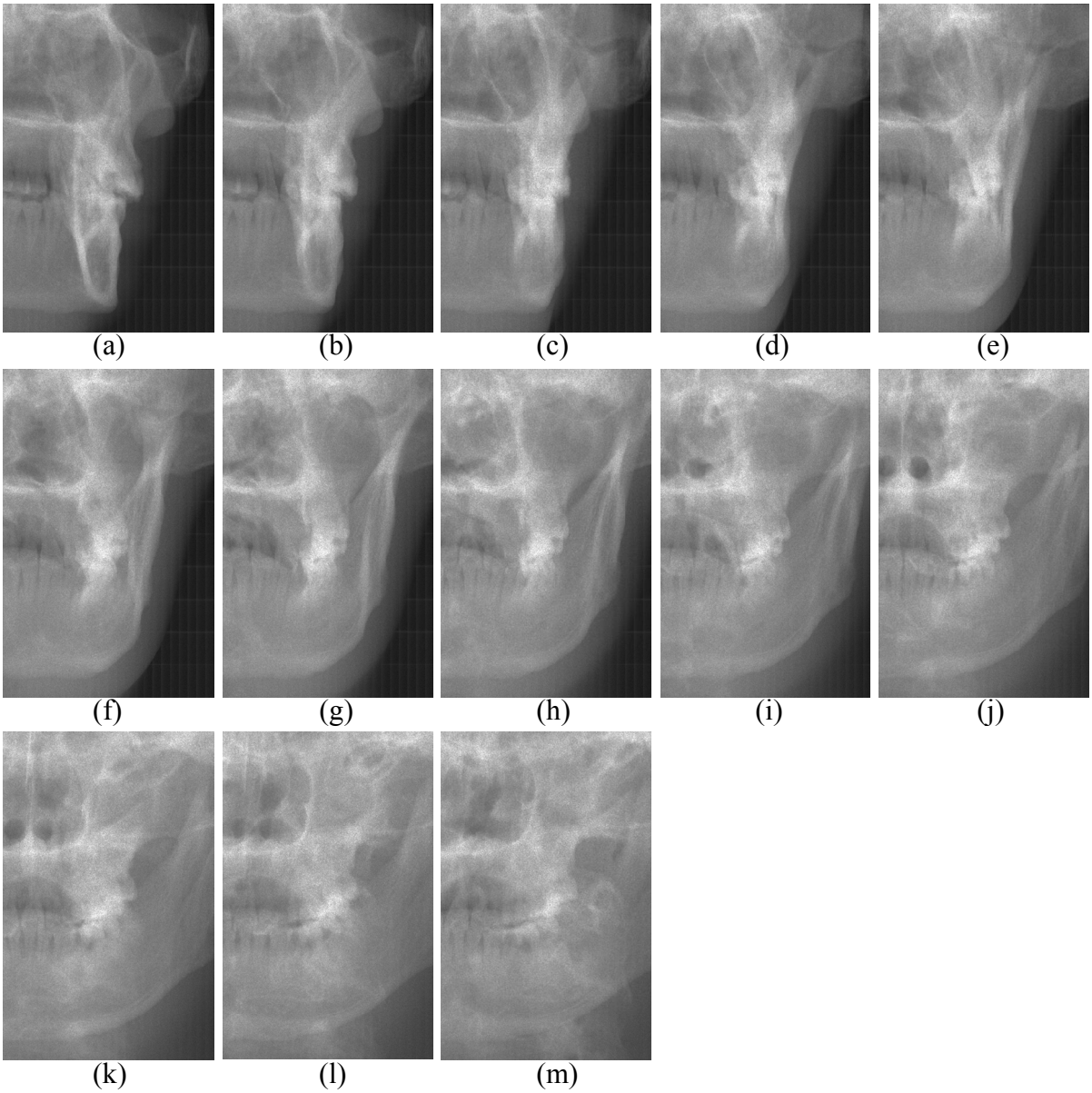

Fig. 8 Samples of (-log of) irregular projection images selected from real data.

To reconstruct cross-sectional images $\boldsymbol{\mu}$ from the projection data $\boldsymbol{y}$, we used the ordered-subset convex (OSC) algorithm[9] which is given by

$$\mu_j^{n,k+1} = \mu_j^{n,k} + \mu_j^{n,k} \frac{\sum_{i \in S_k} a_{ij} \left(1 - \frac{y_i}{b_i \exp(-[A\boldsymbol{\mu}^{n,k}]_i)} \right) b_i \exp(-[A\boldsymbol{\mu}^{n,k}]_i)}{\sum_{i \in S_k} a_{ij} [A\boldsymbol{\mu}^{n,k}]_i b_i \exp(-[A\boldsymbol{\mu}^{n,k}]_i)}$$

where S_k contains the projections in subset *k*, and $\cup S_k$ equals to all projections, A denotes the system matrix whose elements are a_{ij}. In this work, the number of subset was 156. The number of iterations was 2. The reconstructed volume

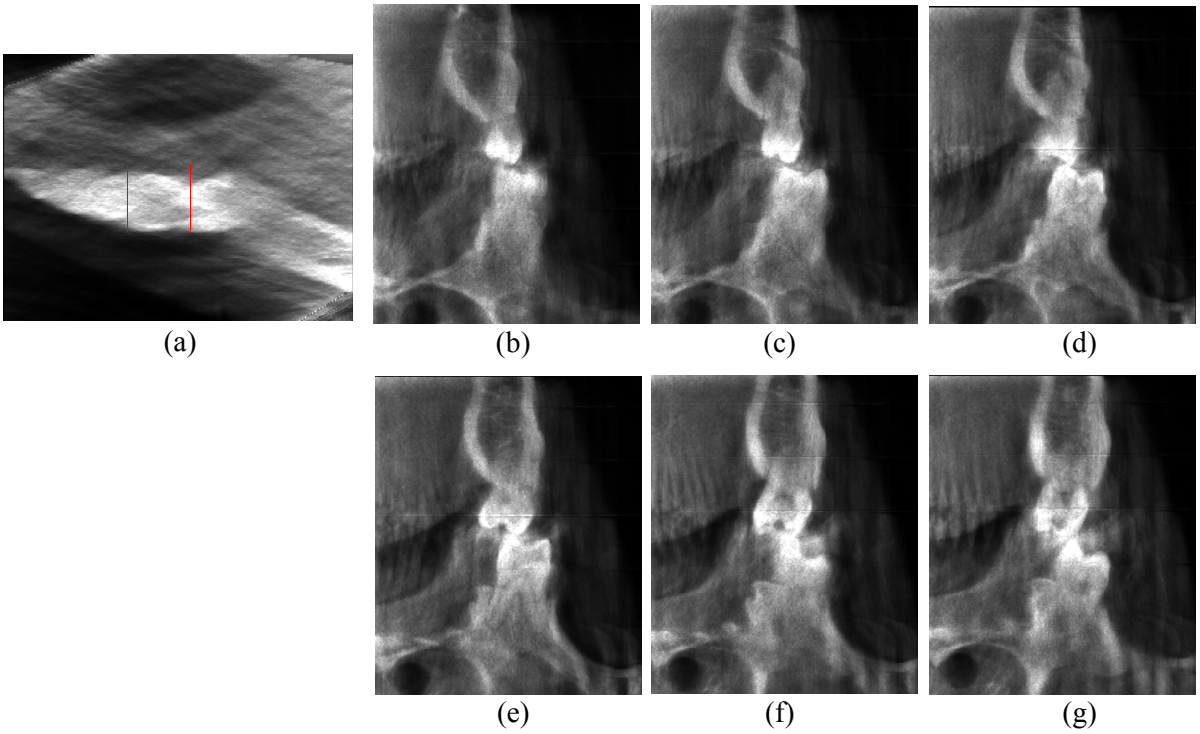

Fig.9. Cross-sectional images acquired by the proposed method from a panoramic scanner: (a) an axial slice (The two line segments denote the positional range of the cross-sectional slices shown in (b) thru (g)); (b)-(g) samples of reconstructed cross-sectional slices with the slice interval of 2.72 mm.

had the size of 512×512×512 with the voxel size of 0.272×0.272×0.272mm^3. The Siddon's ray-tracing method[10] was used to perform projection and backprojection.

Fig. 9 shows an axial slice of a molar region and several cross-sectional slices which demonstrate the performance of our proposed method to acquire a 3D image using the panoramic unit with a narrow detector. The image size was cropped to 256×384×328 for the ease of view. As shown in Figs. 9(b)-(g), the cross-sectional slices obtained by our method show useful 3D structures of the object that is much larger than the width of the narrow detector originally designed for conventional panoramic imaging. Finally, since the detector consists of 10 small longitudinal blocks each of which has 150×48 detector cells, there exist some distortions in the sensitivity of the detector cells along the border of two adjacent blocks, which results in minor line artifacts in reconstructed images as shown in Figs. 9(b)-(g). We are currently developing a calibration method to reduce the distortions along the border of the two adjacent blocks.

One factor that can affect the image quality is the speed of angular and linear movements of the suspension arm; the faster the suspension arm moves, the blurrier the image gets. The reconstruction algorithm used in this work assumes that the projection data are acquired in a step-and-shoot mode. In other words, it is assumed that both the object and the suspension arm do not move during the acquisition of a projection image. Unfortunately, however, our continuous acquisition mode does not allow a step-and-shoot mode. In our case, a projection image is generated every 5 milliseconds during which both the detector and X-ray source move. If the speed of angular and linear movements is considerably low, therefore the acquisition takes longer, it can be approximated to a step-and-shoot mode.

So far we have considered a uni-directional raster scan for our data acquisition scheme where the scan is performed in one direction as illustrated in Fig. 10(a). While this acquisition scheme can simplify the motion of the suspension arm, it results in long scanning time due to the blanking time during which the arm sweeps back to the next starting point of acquisition for the next irregular projection image. To reduce the scan time, thereby reducing the patient's motion artifact, we acquired the data using a bi-directional raster scan mode as illustrated in Fig. 10(b).

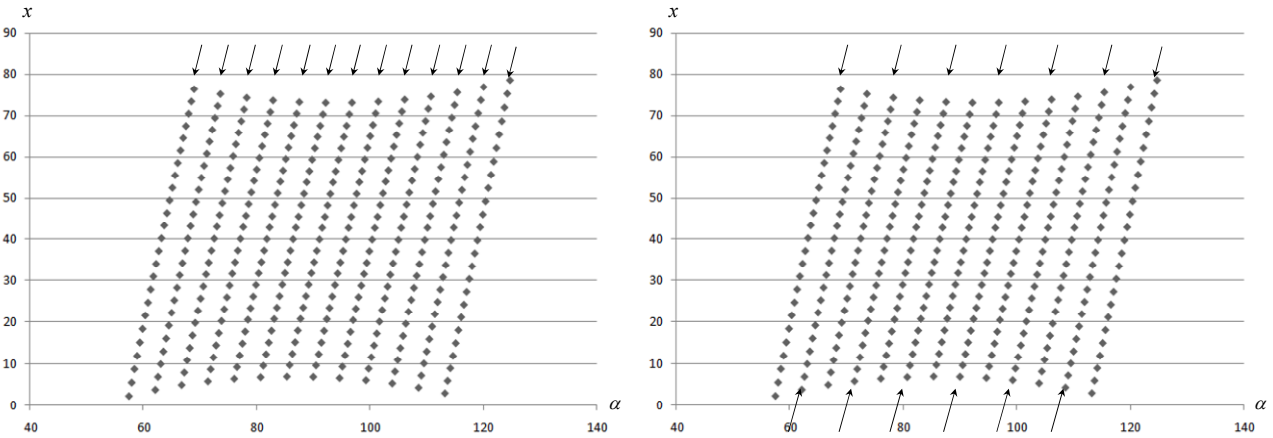

(a) (b)

Fig.10. Two different modes of raster scan for data acquisition. (a) Uni-directional raster scan. (b) Bi-directional raster scan. The arrow indicates the starting point of each scan.

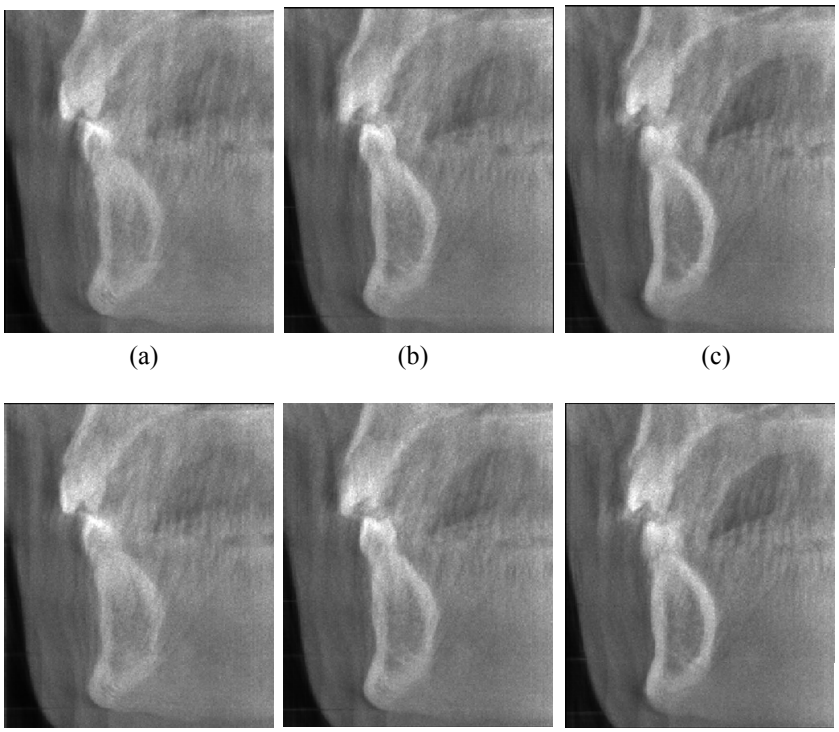

(a) (b) (c)

(d) (e) (f)

Fig.11. Cross-sectional images acquired by the proposed method from a panoramic scanner using: (a)-(c) Uni-directional raster scan. (d)-(f) Bi-directional raster scan. The slice interval is of 2.72 mm.

Fig. 11 compares the reconstructed images obtained from uni-directional raster scan (first row) and bi-directional raster scan (second row). A closer look reveals that the bi-directional raster scan makes the results slightly blurrier. This is presumably due to the fact that the moving pattern of the suspension arm changes whenever the scan direction changes in the bi-direction raster scan mode. Nevertheless, in order to minimize the patient's motion artifact, a fast scan is still useful in practice.

4. DISCUSSION AND CONCLUSION

We have proposed and validated a new method to perform CT imaging using a conventional panoramic X-ray scanner with a narrow detector. The method has great potential to enable existing panoramic X-ray scanners to have an additional CT's function of providing useful tomographic images. Although our proposed method has a major advantage of providing useful cross-sectional images with an inexpensive narrow detector, it has some limitations.

Since the acquisition is performed with a small angular coverage (around 40-60 degrees), the reconstructed images have limited angle artifact which degrades the quality of reconstruction. Further investigations are needed to reduce this artifact in reconstruction, such as some techniques mentioned in Ref 11.

In dental practice, panoramic scanners provide a wide field of view about the jaw. The 3-D image acquired by a panoramic scanner using proposed method shows the structure of a small region of interest (ROI) only. Meanwhile, the acquired projection data also contain the information on the non-ROI structure. Reconstructing ROI only from the acquired projection data is challenging[12]. We are currently investigating ROI reconstruction methods to restore cross-sectional slices from irregular projection images.

Though the MBIR used in this work has great potential to provide excellent image quality, it suffers from long computation time. To overcome this problem and make our proposed method usable in practice, it is necessary to improve our method so that it can significantly reduce the computation time for the MBIR. We are currently investigating several ways of accelerating the MBIR such as down-sampling the projection data (since the resolution of the dental projection data is very high) and using graphics processing units (GPUs) to reduce the computational load of forward and backward projections[13]. The irregular projection images could also be rebinned to conventional parallel beam projection images so that existing fast reconstruction algorithms can be directly used.

In this work, we assumed that the scanner was perfectly calibrated. In practice, however, the calibration process is always less than ideal. This is especially true for our proposed method where the arm moves with a complex trajectory and it is very difficult to measure the geometrical parameters which are closely related to the system matrix A. In order to make our method more practical, the development of accurate geometrical calibration method is needed.

In conclusion, our proposed method provides a new way of acquiring cross-sectional images about a relatively large object using a conventional panoramic scanner with a narrow detector.

5. ACKNOWLEDGEMENTS

This work was supported by Basic Science Research Program of the National Research Foundation of Korea (NRF) funded by the Ministry of Education under Grant NRF-2011-0014325 for S.-J. Lee, the Le Quy Don Technical University under Grant 3331/QD-HV/2013 and the Vietnam National Foundation for Science and Technology Development (NAFOSTED) under Grant 102.01-2013.42 for V.-G. Nguyen.

REFERENCES

[1] Müller, T., "Methods, apparatuses and imaging mode for tomographic imaging," *US Patent* 6470069 (2002).
[2] Frosio, I. and Borghese, N.A., "Tomosynthesis through a time delay integration sensor," *IEEE Nuclear Science Symposium and Medical Imaging Conference*, 3823-3825 (2007).
[3] Siltanen, S., Jouhikainen, "Method for producing a three-dimensional digital X-ray image," *US Patent* 7813469 (2010).
[4] Kolehmainen, V., Vanne, A., Siltanen, S., Jarvenpaa, S., Kaipio, J. P., Lassas, M. and Kalke, M., "Bayesian inversion method for 3D dental X-ray imaging," *Elektrotechnik & Informationstechnik* **124**, 248–253 (2007).
[5] Cederlund, A., Kalke, M. and Welander, U, "Volumetric tomography – a new tomographic technique for panoramic units," *Dentomaxillofacial Radiology*, **38**, 104-111 (2009).
[6] Hyvönen, N., Kalke, M., Lassas, M., Setälä, H. and Siltanen, S. "Three-dimensional dental X-ray imaging by combination of panoramic and projection data," *Inverse Problems and Imaging*, **4**(2), 257-271 (2010).
[7] Thibault, J.-B., Sauer, K.D., Bouman, C.A., Hsieh, J. "A three-dimensional statistical approach to improved image quality for multislice helical CT," *Medical physics*, **34**, 4526-4544 (2007)

[8] Hsieh, J, Nett, B, Yu, Z, Sauer, K, Thibault, J.-B., Bouman, C.A., "Recent Advances in CT Image Reconstruction", *Current Radiology Reports*, **1**, 39-51, 2013.
[9] Beekman, F. J. and Kamphuis, C., "Ordered subset reconstruction for X-ray CT," *Physics in Medicine and Biology* **46**, 1835-1844 (2001).
[10] Siddon, R.L., "Fast calculation of the exact radiological path for a three-dimensional CT array," *Medical Physics*, **12**, 252-255 (1985).
[11] Zhang, Y., Chan, H. -P., Sahiner, B., Wei, J., Ge, J., Zhou, C., and Hadjiiski, L. M., "Artifact reduction methods for truncated projections in iterative breast tomosynthesis reconstruction," *J. Comput. Assist. Tomogr.*, **33**, 426-435 (2009).
[12] Faridani, A., Ritman, E.L., and Smith., K.T., "Local tomography," *SIAM Journal on Applied Mathematics*, **52**, 459–484 (1992).
[13] Nguyen, V. -G., Jeong, J., and Lee, S. -J., "GPU-accelerated iterative 3D CT reconstruction using exact ray-tracing method for both projection and backprojection," *IEEE Nuclear Science Symposium and Medical Imaging Conference*, (2013).